Global Sensitivity of Penman-Monteith Reference Evapotranspiration to Climatic Variables in Mato Grosso, Brazil

Marlus Sabino and Adilson Pacheco de Souza *

Posted Date: 3 August 2023

doi: 10.20944/preprints202308.0210.v1

Keywords: Sobols' method; Climate change; Amazon; Cerrado

Article

Global Sensitivity of Penman-Monteith Reference Evapotranspiration to Climatic Variables in Mato Grosso, Brazil

Marlus Sabino [1] and Adilson Pacheco de Souza [1,2,*]

[1] Postgraduate Program in Environmental Physics, Institute of Physics, Federal University of Mato Grosso (UFMT), Cuiabá, MT, Brazil; marlussabino@gmail.com (M.S.)
[2] Institute of Agricultural and Environmental Sciences, Federal University of Mato Grosso (UFMT), Sinop, MT, Brazil; adilson.souza@ufmt.br (A.P.S.)
* Correspondence: pachecoufmt@gmail.com; Tel.: +5566981363805

Abstract: Understanding how climatic variables impact the reference evapotranspiration (ET_0) is essential for water resource management, especially considering potential fluctuations due to climate change. Therefore, we used the Sobol method to analyze the spatiotemporal variations of Penman-Monteith ET_0 sensitivity to the climatic variables: downwards solar radiation, relative humidity, maximum and minimum air temperature, and wind speed. The Sobol's indices variances were estimated by Monte Carlo integration, setting the sample limits to 2.5 and 97.5 percentiles of the daily data of 33 automatic weather stations located in the state of Mato Grosso, Brazil. The results of the Sobol analysis indicate considerable spatiotemporal variations in the sensitivity of ET_0 to climatic variables and their interactions. The dominant climatic variable responsible for ET_0 fluctuations in Mato Grosso is incident solar radiation, which has a more significant impact in humid environments, as observed in the areas of the Amazon biome in the state. Air relative humidity and wind speed have higher sensitivity indices during the dry season in the areas of the Cerrado biome (Savanna) in Mato Grosso. Our findings show that changes in solar radiation, relative humidity, and wind speed cannot be ignored when analyzing changes in reference evapotranspiration.

Keywords: Sobol's method; Climatic change; Amazon; Cerrado

1. Introduction

Reference evapotranspiration (ET_0) is defined as the potential evapotranspiration of a hypothetical well-watered and actively growing grass surface of uniform height [1]. Understanding the mechanism of ET_0 is crucial in agricultural and hydrological studies and projects at local, regional, or global scales [2–8], as it plays an essential role in the hydrological cycle.

Given the importance of ET_0, different methods have been developed to model it, which, based on their fundamental factors, can be divided into three categories: mass transfer, radiation, and temperature equations [9–14]. The Penman-Monteith equation is a physical model that combines mass transfer and radiation methods and is the recommended methodology recommended by the FAO to estimate reference evapotranspiration [1].

The FAO-Penman-Monteith method is jointly determined by climatic variables such as downwards solar radiation (SRD), relative humidity (RH), maximum and minimum temperature (Tmax and Tmin), and wind speed (WS). For instance, affected by climate change, an increase in ET_0 can lead to an increase in the frequency, duration, and severity of drought [15,16], resulting in a lower water supply available in lakes, reservoirs, and groundwater [17,18]. However, in many hydrological and water resources climate change analyses only the changes in temperature and precipitation are investigated using temperature-based ET_0 estimation methods [19–21], which could lead to inaccuracies by not considering changes in solar radiation, wind speed, and relative humidity.

Sensitivity analysis are methodologies that allow for evaluating the relationships between the input and output variables of a system [22]. The methodology has been widely employed in

 doi:10.20944/preprints202308.0210.v1

environmental sciences, ecology, and hydrology, among others [23]. In studies related to evapotranspiration, sensitivity analysis enables the inspection of the impact that changes in climate variables have on the ET_0 fluctuation, as well as the identification of its dominant variables [24–26].

The sensitivity analysis methodologies are commonly divided into local sensitivity analysis (LSA) and global sensitivity analysis (GSA). Although local sensitivity analysis has been widely used to identify the influence of climatic variables on ET_0 [27–31], the LSA method has no self-verification and only reflects the local effects of individual variables [32]. On the other hand, global sensitivity analysis has the advantage of estimating the impact of all inputs and their combined effects on output changes [33,34]. The Sobol method is a GSA method based on variance decomposition analysis that provides a more robust performance than nonlinear models like the FAO-Penman-Monteith ET_0 [35,36]. Additionally, the Sobol method can assess the impact of uncertainties in the variables by encompassing their entire range of values, thus providing more information to quantify the influence of meteorological variables on ET_0.

Among the Brazilian territory, the state of Mato Grosso stands out for its vast territorial area, which encompasses three biomes: the Pantanal wetlands, savanna formations (Cerrado), and the Amazon rainforest, as well as two climate types: Aw climate (tropical savanna climate) and Cwa (tropical climate) [37]. The main economic activity in the state is agricultural production, with Mato Grosso being the largest grain producer in Brazil [38]. However, despite the high demand for water resources and the potential for expanding irrigated agriculture systems, there is still a lack of research focused on the impacts that changes in climate variables have on the fluctuation of evapotranspiration in the state of Mato Grosso [39,40].

Therefore, as it is critical to identify the dominant climatic variables that control ET_0 in the region to better plan the use of water resources, this study has three objectives: i) Analyzing the spatiotemporal variations in ET_0 and its related climatic variables (SRD, RH, Tmax, Tmin, and WS) in the state of Mato Grosso, Brazil; ii) Determining and discussing the sensitivity of ET_0 to the climatic variables; iii) Determining the dominant climatic variable attributed to ET_0 variability in the region.

2. Materials and Methods

2.1. Study Area and data

The state of Mato Grosso is located between the coordinates 06°00'S, 19°45'S and 50°06'W, 62°45'W and has a large territorial extension, with an area of 903,202,446 km², which represents 10.61% of the territory of Brazil. Climate-wise, the state has two well-defined seasons: the wet season, from October to April, and the dry season, from May to September. The total annual precipitation ranges from 1,200 to 2,000 mm, with higher levels in the north and east-north regions, as well as in areas with altitudes close to 800 m. The predominant climate is classified as Aw (Tropical savanna climate) and Cwa (tropical climate) according to Köppen classification [37].

The study used daily time-series data from 2008 to 2020 of the climatic variables: downwards solar radiation (SRD in MJ m^{-2} day^{-1}), relative air humidity (RH in %), maximum air temperature (Tmax in °C), minimum air temperature (Tmin in °C), and mean wind speed at 2 meters (WS in m s^{-1}). These data were collected from 33 automatic weather stations (AWS) belonging to the National Institute of Meteorology (INMET), distributed throughout Mato Grosso, Brazil (Table 1, Figure 1).

Table 1. INMET automatic weather stations (AWS) in the Mato Grosso, Brazil.

AWS	AWS name	Biome	Lat.[1]	Lon.[2]	Alt.[3]
A-901	Cuiabá	Cerrado	-15.56	-56.06	242
A-902	Tangará da Serra	Amazon	-14.65	-57.43	440
A-903	São José do Rio Claro	Cerrado- Amazon	-13.45	-56.68	340
A-904	Sorriso	Cerrado- Amazon	-12.56	-55.72	379
A-905	Campo Novo do Parecis	Cerrado	-13.79	-57.84	525
A-906	Guarantã do Norte	Amazon	-9.95	-54.90	284
A-907	Rondonópolis	Cerrado	-16.46	-54.58	290

Preprints (www.preprints.org) | NOT PEER-REVIEWED | Posted: 3 August 2023 doi:10.20944/preprints202308.0210.v1

A-908	Água Boa	Cerrado	-14.02	-52.21	440
A-910	Apiacás	Amazon	-9.56	-57.39	218
A-912	Campo Verde	Cerrado	-15.53	-55.14	748
A-913	Comodoro	Cerrado	-13.71	-59.76	577
A-914	Juara	Amazon	-11.28	-57.53	263
A-915	Paranatinga	Cerrado	-14.42	-54.04	477
A-916	Querência	Amazon	-12.63	-52.22	361
A-917	Sinop	Cerrado- Amazon	-11.98	-55.57	367
A-918	Confresa	Cerrado- Amazon	-10.64	-51.57	233
A-919	Cotriguaçu	Amazon	-9.91	-58.57	265
A-920	Juína	Amazon	-11.38	-58.77	365
A-921	São Felix do Araguaia	Cerrado	-11.62	-50.73	201
A-922	Vila Bela da Santíssima Trindade	Amazon	-15.06	-59.87	213
A-924	Alta Floresta	Amazon	-10.08	-56.18	292
A-926	Carlinda	Amazon	-9.97	-55.83	294
A-927	Brasnorte (Novo Mundo)	Cerrado- Amazon	-12.52	-58.23	426
A-928	Nova Maringá	Cerrado- Amazon	-13.04	-57.09	334
A-929	Nova Ubiratã	Cerrado- Amazon	-13.41	-54.75	466
A-930	Gaúcha do Norte	Cerrado- Amazon	-13.18	-53.26	376
A-931	Santo Antônio do Leste	Cerrado	-14.93	-53.88	664
A-932	Guiratinga	Cerrado	-16.34	-53.77	525
A-933	Itiquira	Cerrado	-17.17	-54.50	593
A-934	Alto Taquari	Cerrado	-17.84	-53.29	862
A-935	Porto Estrela	Cerrado	-15.32	-57.23	148
A-936	Salto do Céu	Amazon	-15.12	-58.13	301
A-937	Pontes de Lacerda	Amazon	-15.23	-59.35	273

[1] Lat. = Latitude. [2] Log. = Longitude ; [3] Alt. = Altitude.

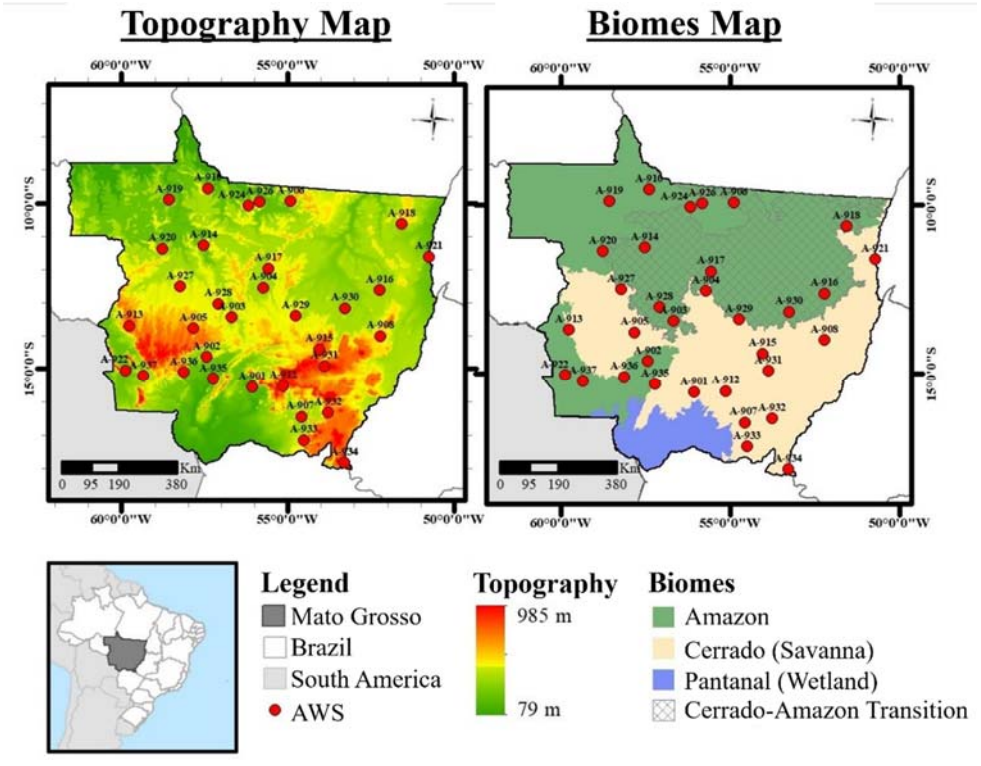

Figure 1: Topographic and biomes maps, and location of INMET Automatic Weather Stations (AWS), in Mato Grosso, Brazil. Numerical identification according to Table 1.

Preprints (www.preprints.org) | NOT PEER-REVIEWED | Posted: 3 August 2023 doi:10.20944/preprints202308.0210.v1

2.2. Reference evapotranspiration (ET0) calculation

The FAO-Penman-Monteith (FAO-PM) is a standardized method recognized by the Food and Agriculture Organization for estimating reference evapotranspiration (ET_0). This method is based on physics and combines physiological and meteorological parameters (i.e., SRD, RH, Tmax, Tmin, and WS) to evaluate ET_0 at a hypothetical grass crop reference surface with an assumed crop height of 0.12 m, a fixed surface resistance of 70 $s \cdot m^{-1}$, and an albedo of 0.23 [1]. In this study, we employ the widely used FAO-56 Penman-Monteith method to calculate ET_0 [1], which is formulated as follows:

$$ET_0 = \frac{0.408\Delta(R_n - G) + \gamma\left(\frac{900}{T+273}\right)WS(es-ea)}{\Delta+\gamma(1+0.34WS)}, \quad (1)$$

where ET_0 = reference evapotranspiration (mm d^{-1}), Rn = net radiation at the crop surface (MJ·m^{-2}·day^{-1}), G = soil heat flux density at the soil surface (MJ·m^{-2}·day^{-1}), T = mean daily air temperature at 2 m height (mean value of Tmax and Tmin, °C), WS = wind speed at 2 m height ($m \cdot s^{-1}$), es = saturation vapor pressure (kPa), ea = actual vapor pressure (kPa), Δ = slope of saturation vapor pressure versus air temperature curve (kPa·°C^{-1}) and γ = psychometric constant (kPa·°C^{-1}). The detailed calculations of Rn, Δ, γ and other parameters needed for computing ET_0 were obtained according to the procedure described in [1]. The G values were ignored for daily estimations purposes (G = 0 MJ m^{-2} d^{-1}).

2.3. Sobol's Sensitivity Analysis Method

Sobol's sensitivity analysis method [41] was utilized to evaluate the monthly sensitivity of PET to the five meteorological variables (SRD, RH, Tmax, Tmin, WS). The choice of Sobol's method was based on its ability to perform variance decomposition analysis and its superior performance in sensitivity analysis of nonlinear and nonmonotonic models [35,36,42]. Moreover, this method allows for examining the individual variables and their interactions and their impact on the model outputs [43]. The fundamental concept behind the Sobol's method is to decompose the model function f(X) (Equation 2) into increasing-dimensional summands, as illustrated in Equation 3:

$$Y=f(X)=f(X_1,X_2,\cdots X_d), \quad (2)$$

$$Y=f_0+\sum_{i=1}^{d} f_i(X_i) + \sum_{i<j}^{d} f_{ij}(X_i,X_j)+\cdots+f_{1,2,\cdots,d}(X_1,X_1,\cdots,X_d), \quad (3)$$

where Y indicates the model function f_0 is the mean value and X are function variables. Considering that all the terms in the functional decomposition are orthogonal, the variance of model output Var(Y) can be decomposed as shown in Equations 4 - 6:

$$Var(Y)= \sum_{i=1}^{d} V_i+\sum_{i<j}^{d} V_{ij}+\cdots+V_{1,2,\cdots,d}, \quad (4)$$

$$V_i=Var_{X_i}\left(E_{X_{\tilde{i}}}(Y/X_i)\right), \quad (5)$$

$$V_{ij}=Var_{X_{ij}}\left(E_{X_{\tilde{ij}}}(Y/X_{ij},X_j)\right)-V_i-V_j, \quad (6)$$

where V_i is the contribution to Var(Y) due solely to the effect of X_i, and $V_{i,2,\ldots,d}$ is the contribution to Var(Y) due to interaction of {X_1, X_2,…, X_d}. Subsequently, the first-order index (S_1) (Equation 7), and total-sensitivity index (S_{tot}) (Equation 8) were calculated as:

$$S_1= \frac{V_i}{Var(Y)}, \quad (7)$$

$$S_{tot}= 1-\frac{Var_{X_{\tilde{i}}}}{Var(Y)}, \quad (8)$$

The variances in the above calculation process were estimated by approximate Monte Carlo numerical integration and the specific calculation details for quantifying the sensitivity can be found

Preprints (www.preprints.org) | NOT PEER-REVIEWED | Posted: 3 August 2023 doi:10.20944/preprints202308.0210.v1

in [44]. This study uses quasi-random sequence sampling since it samples points more uniformly along with the Cartesian grids than uncorrelated random sampling [44]. The number of samples for the quasi-random Monte Carlo was set to 20000 monthly simulations in each AWS. The maximum and minimum range of the variables were set as the 2.5 and 97.5 percentiles of the daily observed data of each month per AWS (Supplementary: Tables S1–S5). We chose this approach to avoid setting the ranges based on outliers of the variable.

Since the minimum temperature in the same sample cannot be higher than the maximum temperature, this study adopts the approach suggested by [34,45]. Firstly, we calculate the mean and difference between Tmax and Tmin. Next, Sobol's sequence sampling is performed on the mean temperature and temperature difference. Finally, the minimum and maximum temperatures are restored from the generated samples.

3. Results

3.1. Climatic variables and Penman-Monteith ET0 spatiotemporal distribution

The monthly mean of Solar Radiation (SRD,) relative humidity (RH), maximum and minimum air temperature (Tmax, Tmin), wind speed (WS), and reference evapotranspiration (ET0) at the 33 AWS in Mato Grosso, Brazil are represented by the boxplots in Figure 2. All variables follow a seasonal pattern between wet and dry seasons. Tmax and WS reach their highest mean at the end of the dry season (38.4 ± 1.3 °C and 1.3 ± 0.5 m s^{-1}) while their lowest mean happens at the end of the wet season (33.8 ± 1.3 °C and 0.9 ± 0.3 m s^{-1}). Tmin and RH mean ranges from 14.6 ± 1.0 °C to 20.0 ± 1.0 °C, and 52.6 ± 7.1% to 83.0 ± 2.5%, with a maximum in the wet season and minimum in the dry season. The lowest mean SRD is during the beginning of the dry season (16.2 ± 2.2 MJ m^{-2} d^{-1}) and gradually increases until the end of the dry season when it reaches its highest mean (19.1 ± 1.4 MJ m^{-2} d^{-1}). The beginning of the dry season also exhibits the lowest ET_0 (3.5 ± 0.3 mm d^{-1}). The evapotranspiration demand increases during the dry period reaching its maximum in September (5.0 ± 0.6 mm d^{-1}) and remaining relatively constant during the wet season (about 4.1 ± 0.3 mm d^{-1}).

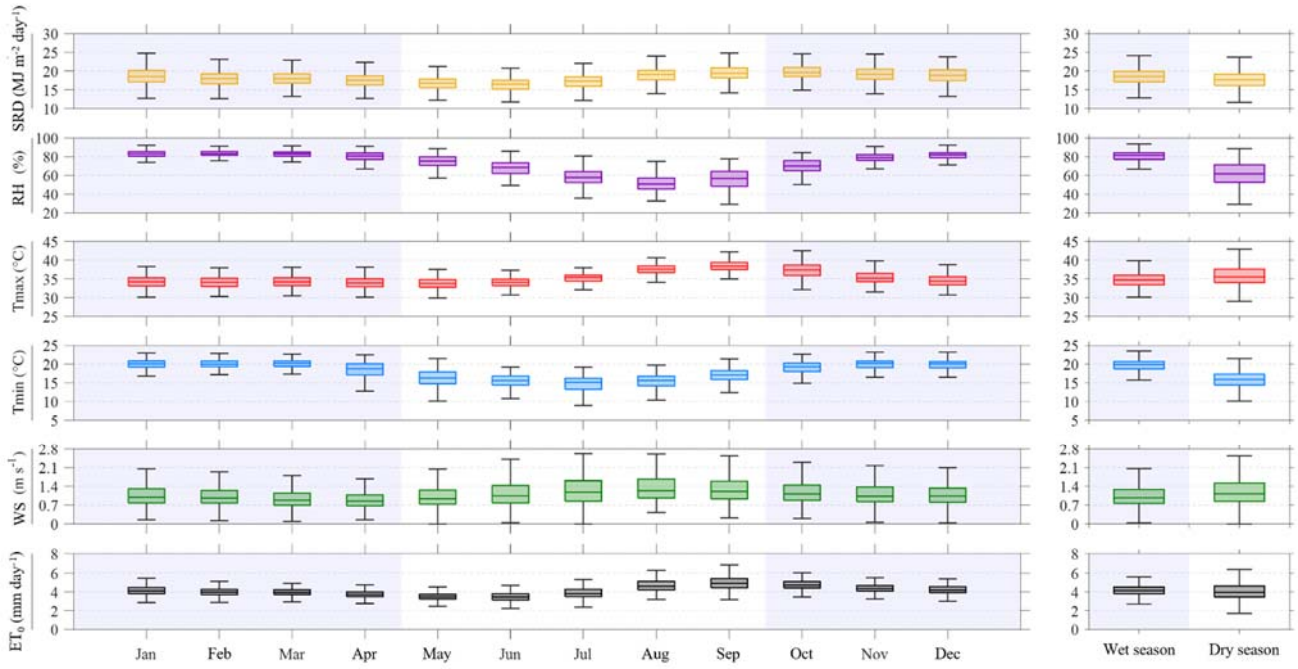

Figure 2: Boxplot showing the monthly variation of Penman-Monteith reference evapotranspiration (ET_0) and its climatic variables obtained on 33 weather stations (AWS) of Mato Grosso, Brazil. (Data series from 2008-2020). Climatic variables: SRD – downward solar radiation; RH - relative humidity; Tmax - maximum air temperature; Tmin - minimum air temperature; WS - wind speed at 2 m. The

Preprints (www.preprints.org) | NOT PEER-REVIEWED | Posted: 3 August 2023 doi:10.20944/preprints202308.0210.v1

top and bottom edge of the box represents the 75th and 25th percentiles. The top and bottom whiskers represent the nonoutlier maximum and minimum. The line inside each box is the median.

The spatial distribution of evapotranspiration and its climatic variables on an annual and seasonal scale is displayed in Figure 3. The results show a zonal variation that follows the distribution of biomes and topography in Mato Grosso. The Amazon region of the state exhibits the lowest values of SRD, Tmax, WS, and ET_0, and the highest values of Tmin and RH. In the Cerrado region, the influence of topography can also be observed in higher altitude areas (southeast part of the state), where there is a decrease in SRD, Tmax, Tmin, and ET_0 compared to the rest of the biome in the state. The spatial distribution of the variables in the state is less evident during the wet season, as there is homogeneity.

in the means of SRD, RH, and Tmin between the two biomes of Mato Grosso.

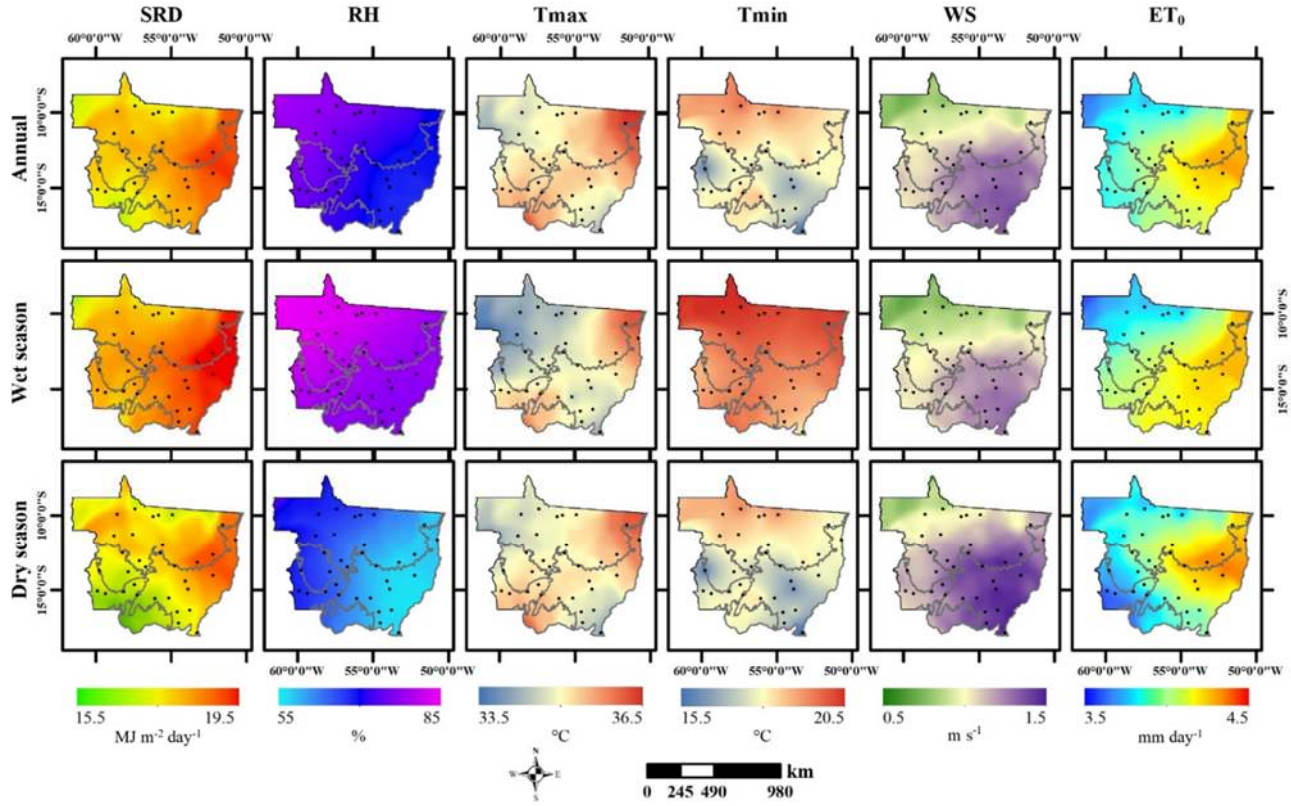

Figure 3: Spatial distribution of Penman-Monteith reference evapotranspiration (ET_0) and climatic variables in the 33 weather stations (AWS) of Mato Grosso, Brazil. (Data series from 2008-2020). Climatic variables: SRD – downward solar radiation; RH - relative humidity; Tmax - maximum air temperature; Tmin - minimum air temperature; WS - wind speed at 2 m. Lines on the map represent the biomes limits, and points represent the automatic weather stations (AWS) of the state of Mato Grosso.

3.2. Sobol sensitivity coefficients spatiotemporal distribution

Figure 4 shows the variation of sensitivity indices for the meteorological variables of ET_0 obtained from the 33 EMAs on an annual and seasonal time scale. Figure 5 presents the monthly variation of these sensitivity indices. Based on the method proposed by [44], the sensitivity indices of the first order (S_1) and total (S_{tot}) can be classified into three levels of sensitivity: insensitive ($S < 0.01$), sensitive ($S \geq 0.01$), and highly sensitive ($S \geq 0.1$). Thus, among the five meteorological variables, ET_0 is highly sensitive to SRD, RH, and WS; sensitive to Tmax; and insensitive to Tmin.

Preprints (www.preprints.org) | NOT PEER-REVIEWED | Posted: 3 August 2023 doi:10.20944/preprints202308.0210.v1

On the annual scale, the sensitivity indices of ET_0 for each variable generally followed the following order: SRD > WS > RH > Tmax > Tmin. Solar radiation (SRD) accounted for the largest variance, representing at least 59% of the total and first-order sensitivity indices during the dry period and reaching an average of 91% during the months of the rainy season. RH and WS explained approximately 8% and 11% of the S_{tot}, and 6% and 9% of the S_1 variation on an annual scale, respectively. RH and WS also alternated as the second most influential variable during the seasonal periods, with RH dominating during the rainy season and WS during the dry season. The temperature variables had a lesser influence on ET_0 in Mato Grosso. Throughout the year, the sensitivity indices of Tmax ranged from 3% to 10%, while Tmin reached a maximum value of approximately 1%.

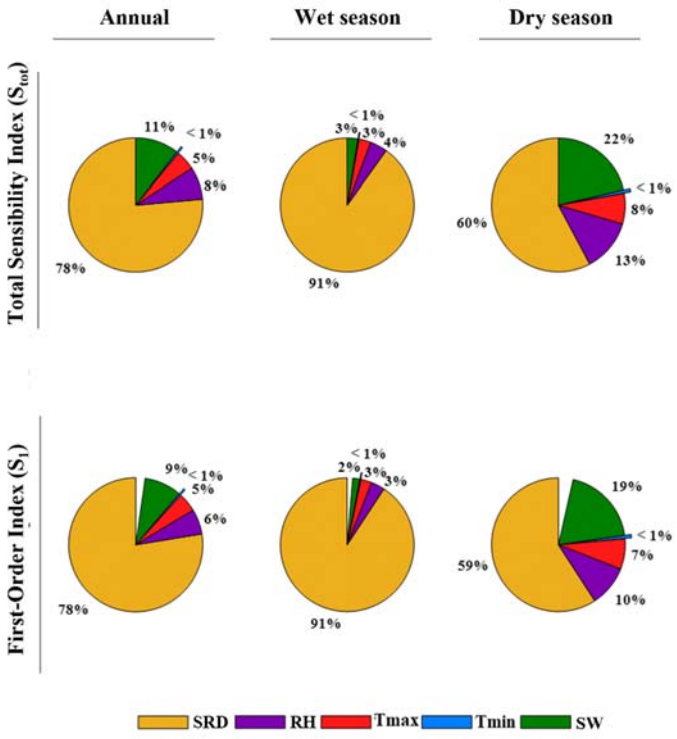

Figure 4: Annual and seasonal of Sobol's first order and total sensitivity indices of the climatic variables used for estimation of Penman-Monteith reference evapotranspiration (ET_0) in the state of Mato Grosso, Brazil. Climatic variables: SRD – downward solar radiation; RH - relative humidity; Tmax - maximum air temperature; Tmin - minimum air temperature; WS - wind speed at 2 m.

Preprints (www.preprints.org) | NOT PEER-REVIEWED | Posted: 3 August 2023 doi:10.20944/preprints202308.0210.v1

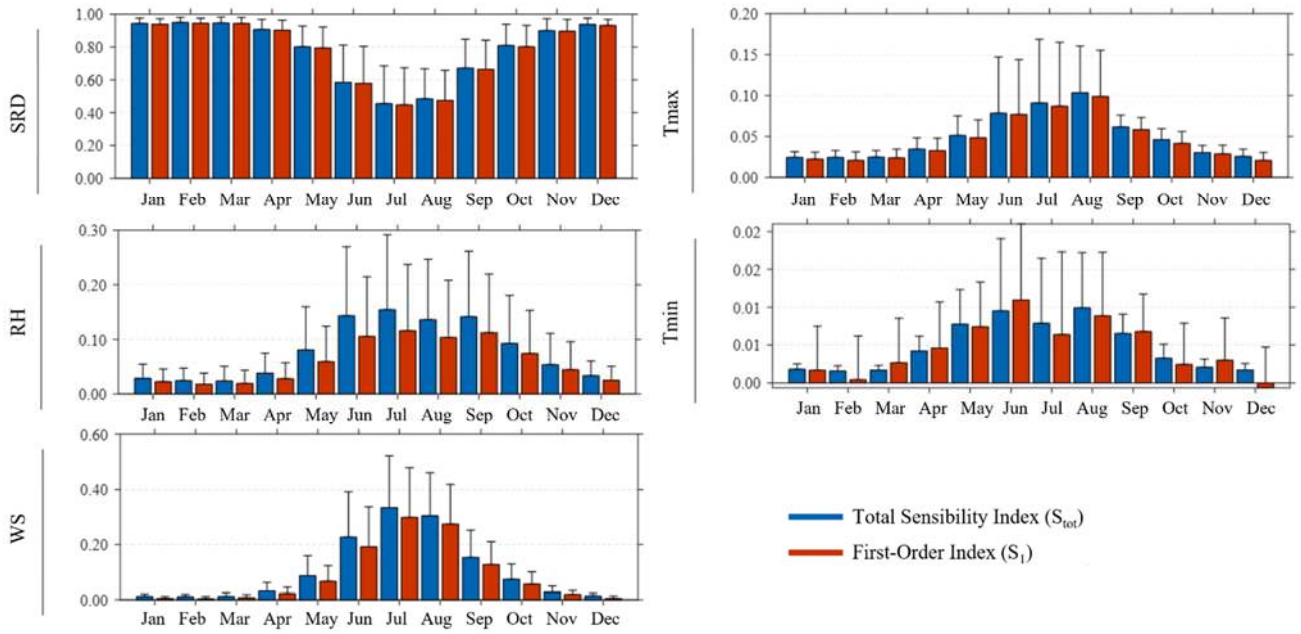

Figure 5: Monthly variations of Sobol's first order and total sensitivity indices of the climatic variables used in the estimation of Penman-Monteith reference evapotranspiration (ET_0) in the state of Mato Grosso, Brazil. Climatic variables: SRD - downward solar radiation; RH - relative humidity; Tmax - maximum air temperature; Tmin - minimum air temperature; WS - wind speed at 2 m. The error bar represents the standard deviation of the indices across the 33 weather stations (AWS) in the state of Mato Grosso, Brazil.

The spatial distributions of the annual and seasonal averages of S_1 and S_{tot} are presented in Figure 6. The results indicate that, in addition to the seasonal behavior, the coefficients exhibit zonal characteristics that resemble the distribution of biomes in the state of Mato Grosso. Although SRD is the dominant variable in determining ET_0 in the state, the influence of radiation differs in the Amazon and Cerrado biomes. While in most of the Amazon region, the sensitivity indices of SRD are on average higher than 80%, in the Cerrado biome, the sensitivity of ET_0 to radiation ranges from 40% to 80%, indicating that RH, WS, and Tmax also influence ET_0 fluctuations in the Cerrado.

Preprints (www.preprints.org) | NOT PEER-REVIEWED | Posted: 3 August 2023 doi:10.20944/preprints202308.0210.v1

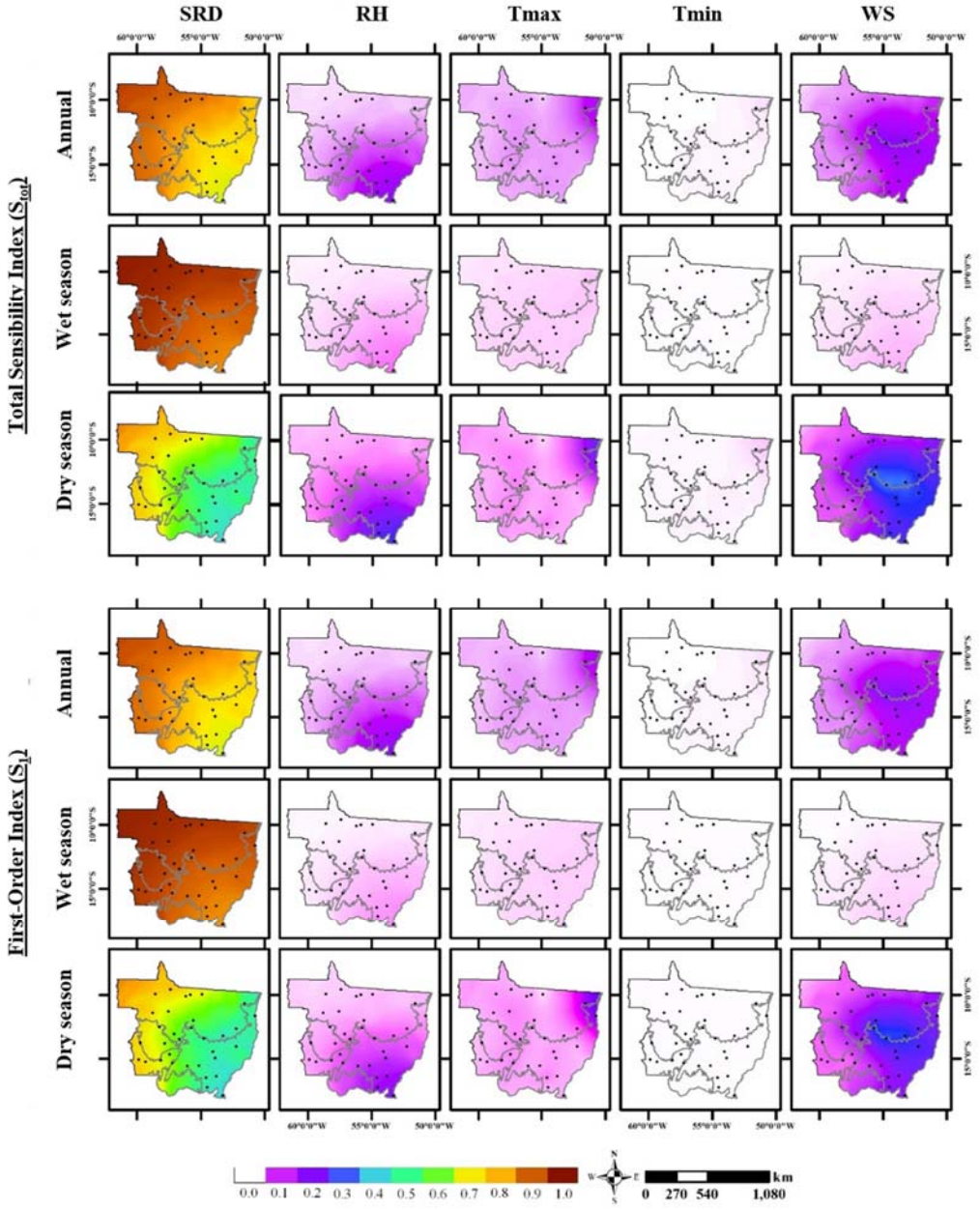

Figure 6: Spatial distribution of Sobol's first order and total sensitivity indices of the climatic variables used in the estimation of Penman-Monteith reference evapotranspiration (ET_0) in the state of Mato Grosso, Brazil, on an annual and seasonal scale. Climatic variables: SRD – downward solar radiation; RH - relative humidity; Tmax - maximum air temperature; Tmin - minimum air temperature; WS - wind speed at 2 m. Lines on the map represent the biomes limits, and points represent the automatic weather stations (AWS) in Mato Grosso.

During the dry season of the Cerrado biome, when the sensitivity indices of SRD are around 50%, it is possible to observe that the second dominant variable varies according to the spatial distribution. In the southeast of the Cerrado, RH becomes the second dominant variable, accounting for 20% to 30% of the ET_0 variation. In the northeastern region of the Cerrado, Tmax becomes the second dominant variable, with approximately 20% to 30% influence. In the central region of the Cerrado, the second dominant variable is WS, with sensitivity indices ranging from 30% to 40%.

4. Discussion

 doi:10.20944/preprints202308.0210.v1

Understanding the causes of ET_0 variations is essential for water resources management and agriculture in Mato Grosso. The results of this study have highlighted the high sensitivity of Penman-Monteith ET_0 to solar radiation in the study area. Overall, the sensitivity of ET_0 to the five meteorological variables in the state can be ranked as follows: SRD > WS ≥ RH > Tmax > Tmin. Although SRD is the dominant climatic variable, explaining 60% to 90% of the ET0 variability throughout the year, the sensitivity of ET_0 the climatic variables, similar to findings in the literature, showed strong indications of spatial variability (Figure 4 6; [25,47,48], with RH playing an important role in determining the spatial and seasonal variations of ET_0 sensitivity indices in Mato Grosso.

In the Mato Grosso Amazon biome portion, higher and relatively constant percentages of relative humidity are observed throughout the year, along with lower values and greater fluctuation of incident radiation measurements (Figure 4 3). The main cause for this pattern is that the Amazon region is characterized as a humid tropical area where convective activity forces the upward movement of moisture, forming a thicker cloud cover compared to the Cerrado region of Mato Grosso [49]. Consequently, in this biome, not only there is a greater attenuation of solar radiation, but there is also a greater reduction in temperature amplitude. This combination of factors could explain why solar radiation is the limiting factor in the evapotranspiration process in the Amazon biome.

These results are consistent with those found in other humid subtropical and tropical areas, such as in the forests of China [48,50], where it is reported that changes in incident solar radiation are the main driving force for ET_0 variability. Similar behavior can also be observed in the Cerrado region of Mato Grosso during the months of the wet season when relative humidity generally exceeds 80%. During this season, maximum temperature and temperature amplitude are lower, and cloud cover increases due to the predominant circulation of the continental equatorial mass (mEc) and the South Atlantic Convergence Zone (ZCAS), which transport moisture from the Amazon to the Cerrado regions (Figure 6) [49,51,52], impacting the solar radiation sensitivity indices.

During the dry season in the Cerrado biome region, the spatial distribution of sensitivity indices indicates three areas of influence analogous to the subdivision of the biome proposed by [51]: Cerrado Meridional (southeastern region of the Mato Grosso Cerrado), Cerrado Central, and Cerrado Setentrional (northeastern region of the Mato Grosso Cerrado). In the Cerrado Meridional region, the occasional incursion of air circulation masses from the polar mass (mP), combined with the topography, leads to increased cloudiness and lower average incident radiation (Figure 6) [52–54]. However, due to lower averages and greater fluctuations in relative humidity (RH) compared to the Amazon biome, an increase in RH sensitivity indices is observed. In the Cerrado Central and Setentrional regions, the reduction in atmospheric humidity caused by the tropical Atlantic mass and the flat topography creates clearer sky conditions [49,51,52,54], thereby reducing fluctuations in incident solar radiation. In this scenario, the increase in sensitivity indices for the variables is linked to their ability to increase water retention in the atmosphere. Therefore, in the Cerrado Setentrional region, where Tmax reaches the highest values in the state, Tmax has greater sensitivity than RH and WS, as it allows for an increase in the saturation vapor pressure deficit. On the other hand, in the Cerrado Central region, where Tmax is lower and WS is higher, wind speed has a greater influence due to disturbances and movement in the atmospheric boundary layer.

These results are consistent with those found by [36,48,55,56] which indicate that atmospheric air circulation directly influences the spatial patterns of global ET0 sensitivity. These authors also agree that high cloudiness and relative humidity conditions are the main factors that increase the sensitivity indices of radiation, while clear sky conditions and low relative humidity increase the sensitivity indices of wind speed. Thus, in arid and semi-arid regions, ET_0 is more sensitive to changes in SRD, WS, and RH variables.

The temperature variables (Tmax and Tmin) generally accounted for less than 10% of ET_0. Although higher temperatures, resulting in reduced RH and increased energy supply to the process, tend to increase ET_0, the effects of Tmax and Tmin on ET_0 sensitivity, as observed in studies by [36,48,55,57], were almost insignificant compared to other factors.

The Sobol method has provided valuable insights for understanding the impact of climatic variables on ET_0. Based on our results, caution should be exercised when making future ET_0 estimates

 doi:10.20944/preprints202308.0210.v1

in Mato Grosso state using formulations that do not account for changes in solar radiation, wind speed, and relative humidity. It is crucial to pay special attention to the estimation of Rs, as it is the dominant variable in Penman-Monteith ET_0 calculations. Furthermore, in the Mato Grosso Cerrado region, particularly during the dry period, the interactions between relative humidity and wind speed cannot be disregarded when determining evapotranspiration using the Penman-Monteith method.

5. Conclusions

The global sensitivity of ET_0 estimated by the Penman-Monteith method to meteorological variables (solar radiation downward- SRD, relative humidity - RH, maximum air temperature - Tmax, minimum air temperature - Tmin, and wind speed at 2 meters – WS) exhibits seasonal and spatial distribution in Mato Grosso state.

Regardless of the period, the dominant variable for evapotranspiration in Mato Grosso is solar radiation (SRD), which has the greatest influence during the rainy season and in humid regions such as the Amazon. The other variables that have a secondary impact on sensitivity follow the ranking of WS > RH > Tmax > Tmin.

ET_0 estimated by the Penman-Monteith method is most sensitive to changes in WS, RH, and Tmax in arid and semi-arid environments, such as the Cerrado during the dry season. However, the sensitivity to RH and WS is higher in the Meridional and Central regions of the Cerrado biome. In contrast, in the Setentrional region, the secondary variable with the highest sensitivity is Tmax.

The meteorological variable Tmin does not significantly influence ET_0 estimated by the Penman-Monteith method in the Mato Grosso state.

The estimation of ET_0 using the Penman-Monteith method for the Mato Grosso state needs to be more accurate and precise data on incident solar radiation (SRD), whether obtained from observed data series at meteorological stations or estimated through gap-filling methods.

Supplementary Materials: The following supporting information can be downloaded at: Table S1: Lower and upper sample limits (Inf - Sup), corresponding to the 2.5th and 97.5th percentiles, of the meteorological variable downward solar radiation (SRD - MJ m-2 day-1) observed in the 33 AWS of Mato Grosso state, Brazil. Table S2: Lower and upper sample limits (Inf - Sup), corresponding to the 2.5th and 97.5th percentiles, of the meteorological variable relative humidity (RH - %) observed in the 33 AWS of Mato Grosso state, Brazil. Table S3: Lower and upper sample limits (Inf - Sup), corresponding to the 2.5th and 97.5th percentiles, of the meteorological variable maximum air temperature (Tmax - °C) observed in the 33 AWS of Mato Grosso state, Brazil. Table S4: Lower and upper sample limits (Inf - Sup), corresponding to the 2.5th and 97.5th percentiles, of the meteorological variable minimum air temperature (Tmin - °C) observed in the 33 AWS of Mato Grosso state, Brazil. Table S5: Lower and upper sample limits (Inf - Sup), corresponding to the 2.5th and 97.5th percentiles, of the meteorological variable Wind speed at 2 m. (WS - m s-1) observed in the 33 AWS of Mato Grosso state, Brazil.

Funding: This study was financed in part by the Coordenação de Aperfeiçoamento de Pessoal de Nível Superior – Brasil (CAPES) – Finance Code 001.

Data Availability Statement: The automatic weather stations (AWS) data used in this study can be accessed by the Instituto Nacional de Meteorologia (INMET) databank website: https://bdmep.inmet.gov.br/#

Conflicts of Interest: "The authors declare no conflict of interest."

References

1. Allen, R. G.; Pereira, L. S.; Raes, D.; Smith, M. Crop Evapotranspiration-Guidelines for Computing Crop Water Requirements-FAO Irrigation and Drainage Paper 56. *Fao, Rome* **1998**, *300* (9), D05109.
2. Liu, B.; Xu, M.; Henderson, M.; Gong, W. A spatial analysis of pan evaporation trends in China, 1955-2000. *J. Geophys. Res.* **2004**, *109*, p. D15102. https://doi.org/10.1029/2004JD004511.
3. McVicar, T.R.; Van Niel, T. G.; LI, L. T.; Hutchinson, M. F.; Mu, X. M.; Liu, Z.H. Spatially distributing monthly reference evapotranspiration and pan evaporation considering[1] topographic influences. *J. Hydrol* **2007**, *338*, p. 196-220. https://doi.org/10.1016/j.jhydrol.2007.02.018.

4. Gu, S.; Tang, Y.; Cui, X.; Du, M.; Zhao, L.; Li, Y.; Xu, S.; Zhou, H.; Kato, T.; Qi, P.; Zhao, X. Characterizing evapotranspiration over a meadow ecosystem on the Qinghai-Tibetan Plateau. *J. Geophys. Res.* **2008**, *113*, p. D08118. https://doi.org/10.1029/2007JD009173.
5. Van der Velde, Y.; Lyon, S. W.; Destouni, G. Data-driven regionalization of river discharges and emergent land cover evapotranspiration relationships across Sweden. *J. Geophys. Res.*: Atmos. **2013**, *118*, p. 2576-2587. https://doi.org/10.1002/jgrd.50224.
6. Araújo Neto, R.A.; dos Santos Nascimento, J.W.; de Oliveira, F.F.; Rebelo, G.R.P.; de Lima Silva, F.D.A.; de Carvalho, A.L., 2020. Models generated by multiple regression in filling meteorological data failures in an automatic meteorological station in Alagoas. *Rev. Geama.* **2020**,*6(2)*, p.4-10.
7. Xiang, K.; Li, Y.; Horton, R.; Feng, H. Similarity and difference of potential evapotranspiration and reference crop evapotranspiration - a review. *Agric. Water Manag.* **2020**, *232*, p. 1-16. https://doi.org/10.1016/j.agwat.2020.106043.
8. Sarnighausen, V.C.R.; Gomes, F.G.; Dal Pai, A.; Rodrigues, S. A. Estimativa da evapotranspiração de referência para Botucatu-SP por meio de modelos de regressão. *RBCLima* **2021**, *28*, p. 766-787. http://dx.doi.org/10.5380/rbclima.v28i0.71569.
9. Penman, H.L. Natural evaporation from open water, bare soil and grass. *Proc R Soc Lond.* **1948**, *193*, p. 120-145. https://doi.org/10.1098/rspa.1948.0037.
10. Thornthwaite, C.W. An approach toward a rational classification of climate. *Geogr. Rev.* **1948**, *38*, p. 55-94. https://doi.org/10.2307/210739.
11. Blaney, H.F.; Criddle, W.D. Determining water requirements in irrigated areas from climatological irrigation data. *Tech. Pap.*, **1950**, *96*, 48 p.
12. Harbeck, G.E. *A Practical Field Technique for Measuring Reservoir Evaporation Utilizing Mass-Transfer Theory*; USGS Professional Paper 272-E:101-105; US Geological Survey: Reston, VA, USA, 1962.
13. Priestley, C.H.B.; Taylor, R.J. On the assessment of the surface heat flux and evaporation using large-scale parameters. *Mon. Weather Rev.* **1972**, *100*, p. 81-92. https://doi.org/10.1175/1520-0493(1972)100<0081:OTAOSH>2.3.CO;2.
14. Guitjens, J.C. Models of Alfalfa Yield and Evapotranspiration. *J. Irrig. Drain. Eng.* **1982**, *108(3)*, p. 212-222. https://doi.org/10.1061/JRCEA4.0001389.
15. Trenberth, K.E.; DAI, A.; Van Der Schrier, G.; Jones, P. D.; Barichivich, J.; Briffa, K. R.; Sheffield, J. Global warming and changes in drought. *Nat. Clim. Chang.* **2013**, *4*, p. 17-22. https://doi.org/10.1038/nclimate2067.
16. Zeng, P., Sun, F., Liu, Y., Feng, H., Zhang, R. and Che, Y. Changes of potential evapotranspiration and its sensitivity across China under future climate scenarios. *Atmos. Res.* **2021**, *261*, p.105763. https://doi.org/10.1016/j.atmosres.2021.105763.
17. Sheffield, J.; Wood, E.F. Projected changes in drought occurrence under future global warming from multi-model, multi-scenario, IPCC AR4 simulations. *Clim Dyn.* **2007**, *31*, p. 79-105. https://doi.org/10.1007/s00382-007-0340-z.
18. Naumann, G.; Alfieri, L.; Wyser, K.; Mentaschi, L.; Betts, R.A.; Carrao, H.; Spinoni, J.; Vogt, J.; Feyen, L. Global changes in drought conditions under different levels of warming. *Geophys. Res. Lett.* **2018**, *45*, p. 3285-3296. https://doi.org/10.1002/2017GL076521.
19. Jha, M.; Pan, Z.; Takle, E. S.; Gu, R. Impacts of climate change on streamflow in the Upper Mississippi River Basin: A regional climate model perspective. *J. Geophys. Res.* **2004**, *109*, p. D09105. https://doi.org/10.1029/2003JD003686.
20. Wang, G.Q.; Zhang, J.Y.; Jin, J.L.; Pagano, T.C.; Calow, R.; Bao, Z.X.; Liu, C.S.; Liu, Y.L.; Yan, X.L. Assessing water resources in China using PRECIS projections and a VIC model. *Hydrol. Earth Syst. Sci.* **2012**, *16*, p. 231-240. https://doi.org/10.5194/hess-16-231-2012.
21. Xu, Y.P.; Pan, S.L.; Fu, G.T.; Tian, Y.; Zhang, X.J. Future potential evapotranspiration changes and contribution analysis in Zhejiang Province, East China. *J. Geophys. Res.-Atmos.* **2014**, *119*, p. 2174-2192. https://doi.org/10.1002/2013JD021245.
22. Song, X.; Zhang, J.; Zhan, C.; Xuan, Y.; Ye, M.; Xu, C. Global sensitivity analysis in hydrological modeling: review of concepts, methods, theoretical framework, and applications. *J. Hydrol* **2015**, *523*, p. 739-757. https://doi.org/10.1016/j.jhydrol.2015.02.013.
23. Saltelli, A.; Aleksankina, K.; Becker, W.; Fennell, P.; Ferretti, F.; Holst, N.; Sushan, L.; Qiongli, W. Why so many published sensitivity analyses are false: a systematic review of sensitivity analysis practices. *Environ. Model Softw* **2019**, *114*, p. 29-39. https://doi.org/10.1016/j.envsoft.2019.01.012.

24. Irmak, S.; Payero, J.O.; Martin, D.L.; Irmak, A.; Howell, T.A. Sensitivity Analyses and Sensitivity Coefficients of Standardized Daily ASCE-Penman-Monteith Equation. *J. Irrig. Drain. Eng.* **2006**, *6*, p. 564-578. https://doi.org/10.1061/(ASCE)0733-9437(2006)132:6(564).
25. Gong, L.; Xu, C.Y.; Chen, D.; Halldin, S.; Chen, Y.D. Sensitivity of the Penman-Monteith reference evapotranspiration to key climatic variables in the Changjiang (Yangtze River) basin *J. Hydrol* **2006**, *329*, p. 620-629. https://doi.org/10.1016/j.jhydrol.2006.03.027.
26. Mosaedi, A.; Ghabaei, M.; Sadeghi, S.H.; Mooshakhian, Y.; Bannayon, M. Sensitivity Analysis of Monthly Reference Crop Evapotranspiration Trends in Iran: A Qualitative Approach. *Theor. Appl. Climatol.* **2015**, *128*, p. 857-873. https://doi.org/10.1007/s00704-016-1740-y.
27. Yang, H.B.; Yang, D.W. Climatic factors influencing changing pan evaporation across China from 1961 to 2001. *J. Hydrol* **2012**, *414*, p. 184-193. https://doi.org/10.1016/j.jhydrol.2011.10.043.
28. Liu, Q.; Yan, C.; Ju, H.; Garré, S. Impact of climate change on potential evapotranspiration under a historical and future climate scenario in the Huang-HuaiHai Plain, China. *Theor. Appl. Climatol.* **2017**, *132*, p. 387-401. https://doi.org/10.1007/s00704-017-2060-6.
29. Lin, P.F.; He, Z.B.; Du, J.; Chen, L.F.; Zhu, X.; Li, J. Impacts of climate change on reference evapotranspiration in the Qilian Mountains of China: historical trends and projected changes. International *J. Climatol.* **2018**, *38*, p. 2980-2993. https://doi.org/10.1002/joc.5477.
30. Jerszurki, D.; De Souza, J.L. M.; Silva, L.D.C.R. Sensitivity of ASCE-Penman–Monteith reference evapotranspiration under different climate types in Brazil. *Clim Dyn.* **2019**, *53(1)*, p. 943-956. https://doi.org/10.1007/s00382-019-04619-1.
31. Zhao, J.; Xia, H.; Yue, Q.; Wang, Z. Spatiotemporal variation in reference evapotranspiration and its contributing climatic factors in China under future scenarios. *Int. J. Climatol.* **2020**, *40*, p. 3813-3831. https://doi.org/10.1002/joc.6429.
32. Saltelli, A.; Aleksankina, K.; Becker, W.; Fennell, P.; Ferretti, F.; Holst, N.; Sushan, L.; Qiongli, W. Why so many published sensitivity analyses are false: a systematic review of sensitivity analysis practices. *Environ. Model Softw* **2019**, *114*, p. 29-39. https://doi.org/10.1016/j.envsoft.2019.01.012.
33. Van Griensven, A.; Meixner, T.; Grunwald, S.; Bishop, T.; Diluzio, M.; Srinivasan, R.A global sensitivity analysis tool for the parameters of multi-variable catchment models. *J. Hydrol* **2006**, *324*, p. 10-23. https://doi.org/10.1016/j.jhydrol.2005.09.008.
34. Xu, Y.P.; Pan, S.L.; Fu, G.T.; Tian, Y.; Zhang, X.J. Future potential evapotranspiration changes and contribution analysis in Zhejiang Province, East China. *J. Geophys. Res.-Atmos.* **2014**, *119*, p. 2174-2192. https://doi.org/10.1002/2013JD021245.
35. Saltelli, A.; Annoni, P.; Azzini, I.; Campolongo, F.; Ratto, M.; Tarantola, S. Variance based sensitivity analysis of model output. Design and estimator for the total sensitivity index. *Comput. Phys. Commun.* **2010**, *181*, p. 259-270. https://doi.org/10.1016/j.cpc.2009.09.018.
36. Zhang, X.; Xiao, W.; Wang, Y.; Wang, Y.; Kang, M.; Wang, H.; Huang, Y. Sensitivity analysis of potential evapotranspiration to key climatic factors in the Shiyang River Basin. *J. Water Clim. Chang.* **2021**, *12(7)*, p. 2875-2884. https://doi.org/10.2166/wcc.2020.225.
37. Souza, A.P.; Mota, L.L.; Zamadei, T.; Martim, C.C.; Almeida, F.T.; Paulino, J. Classificação climática e balanço hídrico climatológico no estado de Mato Grosso. *Nativa* **2013**, *1(1)*, p. 34-43. https://doi.org/10.31413/nativa.v1i1.1334.
38. Dentz, E.V. Produção agrícola no estado do Mato Grosso e a relação entre o agronegócio e as cidades: o caso de Lucas do Rio Verde e Sorriso. *Atelie Geogr.* **2019**, *13(2)*, p.165-186. https://doi.org/10.5216/ag.v13i2.54290.
39. Souza, A.P.; Tanaka, A.A.; Silva, A.C.; Uliana, E.M.; Almeida, F.T.; Gomes, A.W.A.; Klar, A.E. Reference evapotranspiration by Penman-Monteith FAO 56 with missing data of global radiation. *Rev. Bras. Eng. Biossistemas* **2016**, *10(2)*, p. 217-233. https://doi.org/10.18011/bioeng2016v10n2p217-233.
40. Tanaka, A.A.; Souza, A.P.; Klar, A.E.; Silva, A.C.; Gomes, A.W.A. Evapotranspiração de referência estimada por modelos simplificados para o Estado do Mato Grosso. *Pesqui. Agropecu. Bras.* **2016**, *51*, p. 91-104. https://doi.org/10.1590/S0100-204X2016000200001.
41. Sobol, I.M. Sensitivity Estimates for Nonlinear Mathematical Models. *Math. Model. Comput. Expt* **1993**, *4*, p.407-414.
42. Yang, J. Convergence and uncertainty analyses in Monte-Carlo based sensitivity analysis. *Environ. Modell. Softw*. **2011**, *26(4)*, pp.444-457. https://doi.org/10.1016/j.envsoft.2010.10.007.

43. Zhang, K.; Zhu, G.; Ma, J.; Yang, Y.; Shang, S.; Gu, C. Parameter analysis and estimates for the MODIS evapotranspiration algorithm and multiscale verification. *Water Resour. Res.* **2019**, *55*, p. 2211-2231. https://doi.org/10.1029/2018WR023485.
44. Tang, Y.; Reed, P.; Wagener, T.; Van Werkhoven, K. Comparing sensitivity analysis methods to advance lumped watershed model identification and evaluation. *Hydrol. Earth Syst. Sci.* **2007**, *11*, p. 793-817. https://doi.org/10.5194/hess-11-793-2007.
45. Pan, S.; Fu, G.; Chiang, Y. M.; Ran, Q.; Xu, Y. P. A two-step sensitivity analysis for hydrological signatures in Jinhua River Basin, East China. *Hydrol. Sci. J.* **2017**, *62*, p. 2511-2530. https://doi.org/10.1080/02626667.2017.1388917.
46. Yin, Y.; Wu, S.; Dai, E. Determining factors in potential evapotranspiration changes over China in the period 1971–2008. *Chin. Sci. Bull.* **2010**, *55*, p. 3329-3337. https://doi.org/10.1007/s11434-010-3289-y.
47. Zhang, S.; Liu, S.; Mo, X.; Shu, C.; Sun, Y.; Zhang, C. Assessing the impact of climate change on potential evapotranspiration in Aksu River Basin. *J. Geogr. Sci.* **2011**, *21*, p. 609-620. https://doi.org/10.1007/s11442-011-0867-0.
48. Fan, Z. X.; Thomas, A. Decadal changes of reference crop evapotranspiration attribution: Spatial and temporal variability over China 1960–2011. *J. Hydrol* **2018**, *560*, p. 461-470. https://doi.org/10.1016/j.jhydrol.2018.02.080.
49. Arias, P.A.; Fu, R.; Hoyos, C.D.; Li, W.; Zhou, L. Changes in cloudiness over the Amazon rainforests during the last two decades: diagnostic and potential causes. *Clim. Dyn.* **2011**, *37*, p. 1151-1164. https://doi.org/10.1007/s00382-010-0903-2.
50. Stanhill, G., Cohen, S. Global dimming: A review of the evidence for a widespread and significant reduction in global radiation with discussion of its probable causes and possible agricultural consequences. *Agr. Forest Meteorol.* **2001**, *107*, 255-278. https://doi.org/10.1016/S0168-1923(00)00241-0.
51. Nascimento, D.T.F.; Novais, G.T. Clima do Cerrado: dinâmica atmosférica e características, variabilidades e tipologias climáticas. *Élisée* **2020**, *9(2)*, p. e922021.
52. Diniz, F.D.A.; Ramos, A.M.; Rebello, E.R.G. Brazilian climate normals for 1981-2010. *Pesqui. Agropecu. Bras.* **2018**, *53*, p. 131-143. https://doi.org/10.1590/S0100-204X2018000200001.
53. Garreaud, R. Cold air incursions over subtropical and tropical South America: A numerical case study. *Mon. Weather Rev.* **1999**, *127(12)*, p. 2823-2853. https://doi.org/10.1175/1520-0493(1999)127<2823:CAIOSA>2.0.CO;2.
54. Sette, D.M. Os climas do cerrado do Centro-Oeste. *RBCLima* **2005**, *1*, p. 29-42. http://dx.doi.org/10.5380/abclima.v1i1.25225.
55. Taban, H.; Talaee, P.H. Sensitivity of evapotranspiration to climate change in different climates. *Glob. Planet. Change.* **2014**, *115*, p. 16-23. https://doi.org/10.1016/j.gloplacha.2014.01.006.
56. Zhao, J.; Xu, Z. X.; Zuo, D.P.; Wang, X.M. Temporal variations of reference evapotranspiration and its sensitivity to meteorological factors in Heihe River Basin, China. *Water Sci. Eng.* **2015**, *8(1)*, p. 1-8. https://doi.org/10.1016/j.wse.2015.01.004.
57. Zhao, Y.F.; Zou, X.Q.; Zhang, J.X.; Cao, L.; Xu, X.; Zhang, K.; Chen, Y. Spatio-temporal variation of reference evapotranspiration and aridity index in the Loess Plateau Region of China, during 1961-2012. *Quat. Int.* **2014**, *349*, p. 196-206. https://doi.org/10.1016/j.quaint.2014.06.050.